

Electron-induced ordering of the surface structure of $\text{Bi}_2\text{Sr}_2\text{CaCu}_2\text{O}_x$

V. S. Tsoi

Institute of Solid State Physics, Russian Academy of Sciences

(Submitted 11 June 1992)

Zh. Eksp. Teor. Fiz. **103**, 1786–1799 (May 1993)

The (001) surfaces of single crystals of $\text{Bi}_2\text{Sr}_2\text{CaCu}_2\text{O}_x$, which has a complex multicomponent crystal structure, undergo an order-disorder structural transition (surface reconstruction) when bombarded by electrons. The presence or absence of this surface reconstruction depends on the energy of the bombarding electrons in an unusual resonant fashion. In this paper the characteristics of this transition are discussed, and a model is proposed for the surface reconstruction that explains its resonant dependence on electron energy.

INTRODUCTION

Investigations of the structure of the (001) surface of the high-temperature superconductor $\text{Bi}_2\text{Sr}_2\text{CaCu}_2\text{O}_x$ using low-energy electron diffraction^{1–6} and scanning tunnel microscopy^{6–9} have shown that the surface is reconstructed, with a structure close to (1×5) . Just as in the bulk form, a superlattice appears along the direction of the *b*-axis (where *a*, *b*, and *c* are the axes of a tetragonal lattice); this superlattice is apparently incommensurate with the corresponding period of the tetragonal lattice, again as in the bulk form.

Previous researchers have found that irradiation by electrons changes the surface morphology by inducing an order-disorder transition.¹⁰ For a fixed irradiation dose, the sensitivity of the surface to irradiation depends on the electron energy *E* in an unusual “resonant” fashion. When the energy exceeds a certain threshold value, the surface becomes sensitized to irradiation. This sensitivity then increases with energy, reaching a maximum at about 110 eV, and then decreases as the energy is further increased. The sensitivity eventually drops almost to zero at 200 eV, whereupon it becomes almost independent of energy up to 650 eV. This behavior is observed when “perfect” surfaces are irradiated, i.e., surfaces that exhibit easily observed diffraction patterns with the well-known (1×5) structure.

Buzhko and Tsoi¹⁰ showed that irradiation of such a surface by electrons can act like thermal annealing and restore the diffraction pattern; however, this occurs at a relatively high energy ~ 600 eV.

While the importance of such investigations is obvious, it is also obvious that their interpretation will be complicated, and that a variety of possible structural transitions can be induced by irradiating the surface of a multicomponent system with a beam of high-energy particles (or photons). The physical nature of the electron-induced structural transition at the surface of the (001) high-temperature superconductor $\text{Bi}_2\text{Sr}_2\text{CaCu}_2\text{O}_x$ is not understood at the present time (although it is known to be of order-disorder type). The goal of this article is to clarify the nature of this transition by investigating how the appearance of the reconstructed surface under electron bombardment depends on the energy of the irradiating electrons. The data obtained here allow us to establish a number of distinctive features of the process. We then propose a model of the electron-induced surface reconstruction that includes these features, and which explains its unusual (resonant) dependence on the electron energy.¹⁰

EXPERIMENT

Our single-crystal samples of $\text{Bi}_2\text{Sr}_2\text{CaCu}_2\text{O}_x$ had characteristic dimensions $2 \times 3 \times 0.1$ mm³. The surfaces to be studied were obtained by cleaving under the usual conditions, such that the normal to the surface coincided with the direction of the *c* axis. The original single crystals were grown by crucibleless zone melting in an atmosphere of air.¹¹ The stoichiometric composition of the crystals was determined by microscopic x-ray diffraction analysis. The superconducting transition temperature of the original ingot, which was determined by measuring the magnetic susceptibility inductively, was about 86 K, with a transition width of 6 K.

Our measurements were made in an ultrahigh vacuum two-chamber “Riber” apparatus, equipped with the standard devices for rapid introduction of a sample and control of the atomic structure and chemical composition of the surface and residual gases, along with a universal sample manipulator with a system for heating and cooling. The working pressure in the chamber was $\sim 10^{-9}$ torr. The measurements showed that samples could be left in the chamber for several months under these conditions without causing any detectable changes in the diffraction pattern or chemical composition of the surface.

The diffraction pattern was observed after placing the cleaved sample in the high-vacuum chamber and heating it for several minutes at ~ 600 °C. A high-quality diffraction pattern appeared only when the energy of the bombarding electrons was in the range 12–30 eV. In analyzing the quality of the surface morphology, we used the most strongly profiled diffraction pattern, which we observed on a perfect surface at an electron energy of 16 eV. The same electron beam was used to irradiate and to observe the diffraction pattern. The energy of the electrons that drive the structural change in the surface differs considerably from the relatively low energy of the electrons used to analyze the surface morphology. Therefore, it was necessary to eliminate a shift in the electron beam (with a diameter of ≈ 1 mm) along the sample surface as the electron energy changed before recording the structure of the irradiated portion of the surface. This was done in the following way. In the drift region of the electron beam, the magnetic field, which interferes with the rectilinear motion of the electrons, was nulled using three pairs of square coils (with sides ≈ 80 cm) arranged so that their centers coincided and the axes of the coils were mutual-

ly perpendicular. The axis of one pair was directed along the axis of the electron beam, while one of the axes of the two other pairs was placed in the horizontal plane. Using a beam normally incident to the surface, we then recorded the electron diffraction pattern from the (001) surface of a single crystal of $\text{YBa}_2\text{Cu}_3\text{O}_x$ with characteristic dimensions 0.2 to 0.3 mm for electron energies in the interval 10 to 300 eV. By monitoring the currents in the coils, we were able to place the maximum intensity of the diffraction pattern at a previously specified position on the sample in the center of the electron analyzer at various electron energies.

The diffraction pattern was recorded using a computer-controlled system (described in detail in Ref. 12). The image from a fluorescent screen was projected onto a photocathode by a television dissector tube, operating in the counting regime. The dissector has an electromagnetic digital sweep. The system allowed us to measure the local brightness of the optical image of the electronic diffraction pattern on the fluorescent screen with a standard four-grid electron diffractometer. A computer was used to control the system and to collect and process the data in the various regimes (see Ref. 12).

We designed a system for correcting the distortion generated by the optical objective and electromagnetic focusing and deflection systems of the dissector. These corrections were made in the following way: an image was recorded of a control template consisting of a regular square lattice of points. This template was then used to define a transformation from the digital coordinates of a point (m, n) to spatial coordinates (x, y) that transformed the actual image into a template image without distortion. This procedure allowed us to reproduce the true position of a point on the screen with an accuracy of ~ 0.1 mm.

In order to increase the accuracy of our measurements of the angular distribution of electrons, we took into account the fact that the reflections actually fluoresce on a "spherical" surface. This fact is particularly important when the optical axis of the television tube does not coincide with the axis of the electron beam.

A mathematical algorithm and computer program were devised to correct the distortions of the electron-optics recording system. By imaging the diffraction pattern on the spherical fluorescent screen, we were able to transform it into a two-dimensional image of the diffraction pattern in wave-vector space in a plane perpendicular to the direction of propagation of the electron beam. We have presented the data from the diffraction measurements given in this paper in this form.

We studied the electron-induced creation of reconstructed surfaces by recording how the diffraction pattern changed when the sample surface was irradiated by electrons with various energies in the interval 200 to 650 eV. An initially defective surface was prepared in the following way. The surface of an annealed sample on which we observed a high-quality diffraction pattern was irradiated by electrons with energies of 80 eV at a dose of around 10^{-4} K/mm². The diffraction pattern was recorded using 16 eV electrons, with an electron beam current that never exceeded $5 \cdot 10^{-9}$ A. Irradiation by electrons with this energy produced practically no observable degradation of the diffraction pattern;¹⁰ furthermore, this energy was optimal from the point of view of obtaining an intense diffraction pattern with high spatial res-

olution. The electron beam was directed along the normal to the sample surface. This orientation of the normal prevented us from recording the most intense peak in the neighborhood of the (00) reflection (see below), because the apparatus was constructed in such a way that a considerable portion of the central region of the fluorescent screen was blocked by a manipulator, making it impossible for us to observe all the groups of superlattice reflections. However, from the point of view of simplifying the total structural analysis of the surface of such a complicated system (without loss of realism), especially with regard to the feasibility of subsequent numerical analysis, the direction of the incident beam along a symmetrically directed *c*-axis is undoubtedly preferable. As a rule, we recorded individual portions of the diffraction pattern in order to shorten the measurement time and thereby decrease the effect of thermal annealing on the experiment.

RESULTS

The diffraction pattern consists of a number of superlattice reflections located along the *b* axis, with a maximum intensity in the neighborhood of the (00) and $\langle 11 \rangle$ directions. The intensity of the reflections in the neighborhood of the (00) direction are approximately an order of magnitude higher than the intensities of the corresponding reflections in the neighborhood of the $\langle 11 \rangle$ direction. In Fig. 1 we show the measured cross section of the diffraction pattern passing through reflections $(\bar{1}1)$ and $(\bar{1}\bar{1})$, which are located near the points $\pm 0.18 \text{ \AA}^{-1}$, after subtracting the background. The procedure for subtracting the background was as follows. The diffraction pattern was measured twice: once with the electron beam focused onto the surface, and a second time with maximum defocusing. The defocused image was considered to be the background and was subtracted from the focused image after multiplying by a weighting factor that took into account the change in intensity of the electron beam due to defocusing. As a rule, the absolute intensities of the equivalent reflections in the neighborhood of the $\langle 11 \rangle$ points differ somewhat; this is also apparent for the case shown in Fig. 1. A distinctive feature of the diffraction pattern throughout the entire range of energy is the extremely weak intensity of reflections corresponding to the tetragonal (basal) lattice. In Fig. 1 we see a very weak $(\bar{1}0)$ reflection near zero (an analogous situation occurs for the (00) reflection as well). On the same diagram, we show the shape of individual lines calculated in the kinematic approximation, and their sum. In these calculations the line shape was assumed to be Lorentzian, i.e., $I(\mathbf{q}) \propto \{(\mathbf{q} - \mathbf{q}_0)^2 + \beta^2\}^{-1}$, where \mathbf{q} is the wave vector of the reflected electron, \mathbf{q}_0 is one of the vectors of the reciprocal lattice, and the correlation radius is $r_c = 2\pi/\beta$. Practically the same result is obtained when a Gaussian line shape is used. When $r_c = 80 \text{ \AA}^{-1}$ we obtain satisfactory agreement between the calculated line shape and the one observed experimentally (see Fig. 1).

In the initial state, i.e., after irradiation of the sample by electrons with energies 80 eV at a dose of about 10^{-4} K/mm², the superlattice reflections were almost absent. The equilibrium state is the reconstructed (1×5) surface; this surface is also the one that appears as a result of annealing. Because the behavior of the various reflections is similar, we usually based our studies of the dynamics of the reconstruction on measurements of the amplitude of the most intense superlattice reflection, which in Fig. 2 has the coordinate

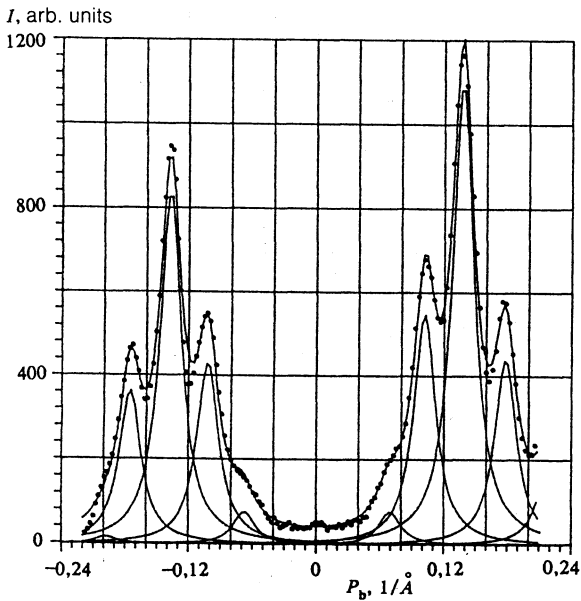


FIG. 1. Measured cross section (points) of the diffraction pattern passing through the reflections (11) and (11), shapes of individual lines calculated in the kinematic approximation, and their sum (the solid curve). The intensity is plotted along the ordinate, the component of the wave vector along the *b* axis along the abscissa.

$\approx 0.14 \text{ \AA}^{-1}$. The dynamic evolution of the superlattice reflections at room temperature is easily seen in the data of Fig. 2. In this figure, we show the time dependence of the relative amplitude of the reflection $A(t)/A_0$, which determines the degree of crystallinity of the structure, along with the quantity $1 - A(t)/A_0$ which determines the degree of imperfection of the structure; $A(t)$ and A_0 denote respectively the amplitude of the reflection after annealing for a time t and the steady-state (equilibrium) amplitude established after a sufficiently long annealing time. The kinetics of this process cannot be described by a single exponential. However, by

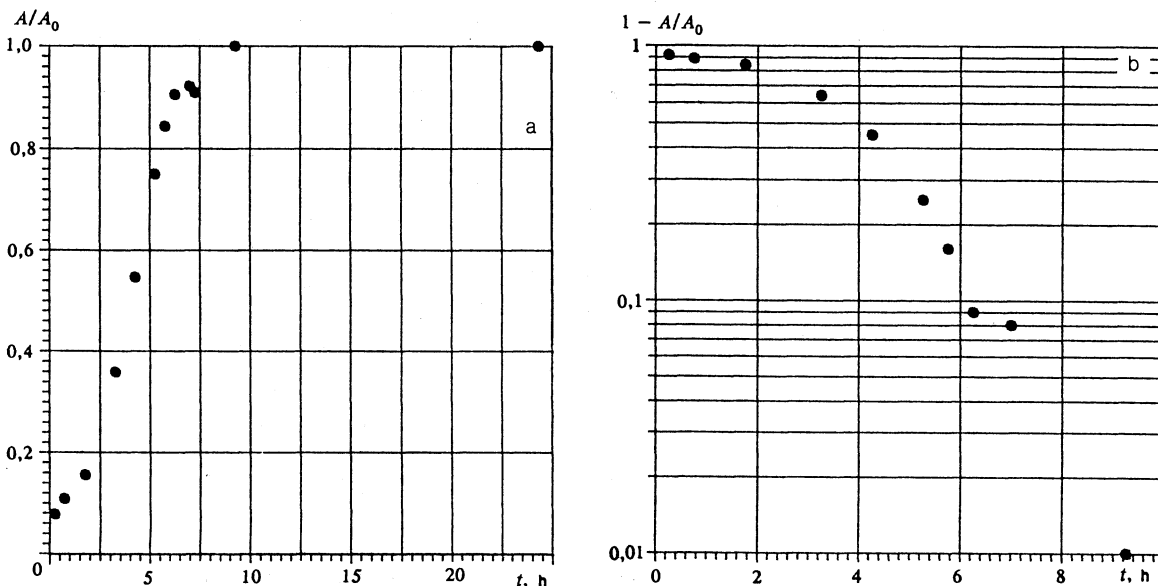


FIG. 2. Dynamic evolution of the amplitude of the superlattice reflections at room temperature.

using exponential dependences we can describe the kinetics adequately by assuming there are two regions of exponential behavior: the first stage of the relaxation and the last, for each of which exponential dependences are appropriate, only with different exponents (see Fig. 2b).

During irradiation by an electron beam, the relaxation process is greatly accelerated. Its dynamics are shown in Fig. 3a, which records the time dependence of the structural imperfection of surfaces irradiated by electron beams with different energies and intensities. This dependence is exponential in form (see Fig. 3a), i.e., $1 - A/A_0 \propto \exp(-\alpha I_s/t)$, where α is a constant determined by the value of the electron energy, I_s is the current flowing through the sample, which is proportional to the intensity of the electron beam, and t is the time.

The relaxation rate depends both on the beam intensity and on its energy; the coefficient in front of the time in the exponent depends almost linearly on intensity (see Fig. 3b). In Fig. 4 we show the experimental dependence of the coefficient α in the exponent on the electron energy (points) and the calculated dependence, assuming the exponential dependence $\alpha \sim \alpha_0 \exp(-E/112.3)$. The coefficient in the exponent is determined by the method of least squares. Agreement between the experimental data and the calculations is satisfactory (see Fig. 4).

It was also established experimentally that irradiation by electrons with energies of 200 eV and higher not only establishes the diffraction pattern with the superlattice reflections, but also causes it to degrade. The features of this process that distinguish it from irradiation by electrons with lower energies are its effective cross section, which is more than an order of magnitude smaller, and its relaxation time after irradiation, which is more than an order of magnitude longer. When the amplitudes of these reflections were suppressed to $\sim 30\%$ of their values by irradiation with 650 eV electrons, the recovery of these amplitudes required about a month. When a defective surface was irradiated by electrons in this energy range, the diffraction pattern changed with time as follows. First, a diffraction pattern with superlattice

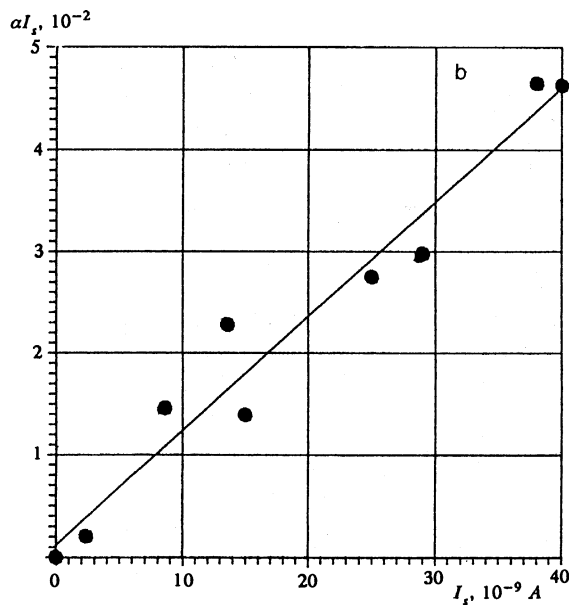
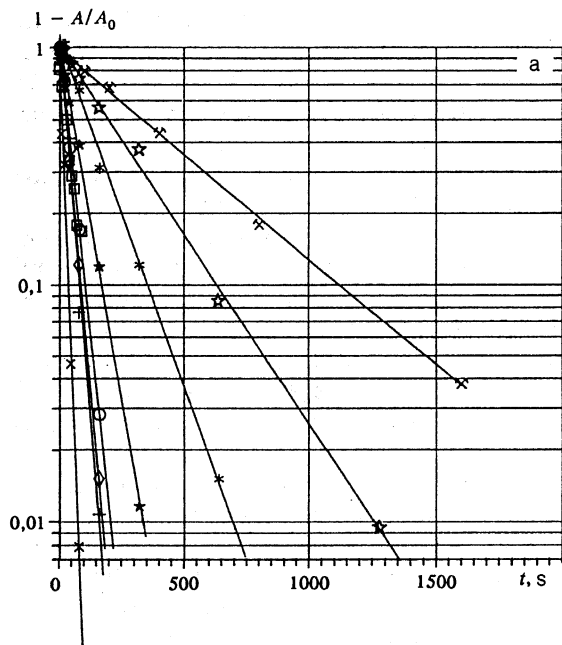


FIG. 3. (a) Dynamic evolution of the amplitude of the superlattice reflections under an electron beam for various values of the current through the sample (in units of 10^{-9} A) and energy E of the electrons (in eV): \star, \ast — $E = 200$ eV, $I_s = 20$ and 31.7 ; $\ast, \circ, \ast, +, \square$ — $E = 300$ eV, $I_s = 2.4, 13.6, 15.0, 29.0$, and 40.0 ; \times — $E = 400$ eV, $I_s = 20.5$; \diamond — $E = 650$ eV, $I_s = 1.3$. (b) Intensity dependence of the exponent αI_s (see Fig. 4a) that determines the relaxation rate on the current I_s flowing through the sample. The electron energy is 300 eV.

reflections was established rapidly; then this pattern slowly degraded, manifested in a decrease of the amplitude of the superlattice reflections.

It is noteworthy that structural changes also take place under the action of an electric field. In our experiments, this field was created by applying an electric potential across the sample. Without dwelling on technical details, we note the following important facts: the surface without a superlattice can exist in a metastable state, and has an appreciable proba-

bility of entering this state when subjected to a negative potential of 50 V relative to ground. In Fig. 5 we show the time dependence of the total quantities, i.e., reflection amplitudes $A(t)$ and diffusive background beneath the reflection, for the case where a structural transformation occurred after we turned off a voltage of 50 V kept across the sample for 1 hour. The solid curve, which gives a picture of the temporal evolu-

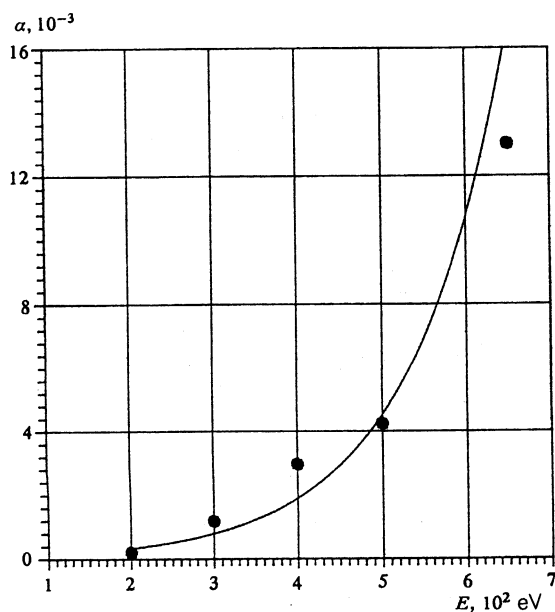


FIG. 4. Dependence on electron energy of the exponent α (see Fig. 4a) that determines the relaxation rate for fixed electron beam intensity.

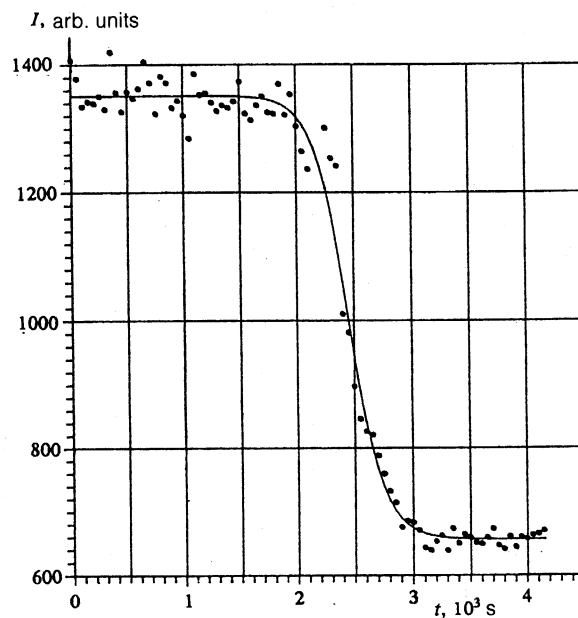


FIG. 5. Time dependence of the intensity of the reflection after removing a voltage from the sample. Along the ordinate we plot the total intensity of the reflections and the background under the reflection in arbitrary units. For $t \geq 3000$ s, the intensity of the reflection equals zero.

tion of the process, has the form $I(t) = 656 + 695/[1 + \exp[(-2450 + t)/150]]$; this adequately describes the experimentally observed time dependence of the reflection intensity. Here t is measured from the time at which the voltage is turned off. We established experimentally that the surface does not always transform to a state without structural reflections after the potential is turned off; sometimes the superlattice is preserved and the diffraction reflections are practically the same intensity as they were before the potential was applied.

DISCUSSION

The data shown in Fig. 1 constitute a precise measurement of a cross section of the diffraction pattern from the (001) surface of $\text{Bi}_2\text{Sr}_2\text{CaCu}_2\text{O}_x$. As such, they allow us to estimate the potential spatial and structural resolution of our apparatus. The effective correlation length equals 80 \AA . Because the apparatus correlation length is approximately equal to this value, all we can say regarding the correlation radius for the superlattice is that it is no smaller than 80 \AA . Measurements show also that the distance between the superstructure reflections remains constant with low accuracy ($\sim 6\%$) exceeding the spectrometer resolution; this indicates in particular that the investigated surface is structurally not perfect.

The relatively rapid rate at which equilibrium is reached on the surface at room temperature indicates that the process of surface reconstruction has a low-energy barrier (see Fig. 2).

A characteristic feature of the structural dynamics of the surface is the existence of a metastable state (see Fig. 5) that becomes available to the surface when a potential of -50 V is applied to the sample with respect to ground. The transition is induced by an electric field that acts on the ions and is localized in the near-surface layer of the sample. Because the distance between the sample and the "ground" is approximately 1 mm and the sample surface is planar, the electric field intensity is small, $\sim 500 \text{ V/cm}$; this suggests that the external electric field by itself has only a small effect on the sample, and can initiate the transition only where the system is "predisposed" to change states, as in ferroelectrics.

Surface reconstruction involves a shift in the positions of the surface atoms. In order for this to occur, it is necessary to supply the atoms with kinetic energy (usually tunnelling effects are negligibly small). Kinetic transfer of energy from an electron to an atom is ineffective when the surface is irradiated by electrons. The true path for supplying an atom with kinetic energy is the following. First, an atom is either ionized or excited as a result of the interaction with an electron. The position of the atom in its new state may then differ from its original position due to the difference between the interaction potentials of the atom in its equilibrium and excited states. The energy necessary for this change in position, whose minimum value determines the threshold energy of this process, is transferred to the atom from the electron that interacts with it. The atom then makes an adiabatic transition to its equilibrium state, thereby acquiring kinetic energy. This process, which explains many features of electron-induced desorption,¹³ can take place by very different routes, e.g., by excitation of neighboring individual atoms or groups of atoms which in turn leads to a shift of a given atom, etc. The change in the kinetic energy of an atom is propor-

tional to the time required for relaxation to the equilibrium state. It depends on the form of the interaction potential between an excited atom and its neighbors, which determines the accelerating force, and is inversely proportional to its mass. It is obvious that this process should play an important role in the electron-induced surface reconstruction discussed here. Note that its sensitivity should be considerably higher than that of the desorption process, because surface reconstruction requires considerably less energy than desorption.

The electron beam affects the surface structure through a mechanism that is electronic in origin. Evidence for this is the fact that the sensitivity to irradiation depends linearly on the beam intensity (see Fig. 3b). Although local heating of the sample due to release of Joule heat can also cause a superlattice to form, this effect is apparently unimportant. In addition to the linear intensity dependence, the sensitivity to electron irradiation exhibits a number of other characteristics that show that this approach is valid, which will be discussed below. An important feature of the relaxation process that also suggests that the interaction is electronic is the threshold dependence of the radiation sensitivity on the electron energy. In the range of energies investigated here, this dependence is satisfactorily described by an exponential. These features point to the following model for the electron-induced surface reconstruction. Atoms are excited by electron bombardment, which is a threshold process. As the excited atoms relax, they acquire kinetic energy and momentum. They transfer this kinetic energy to neighboring atoms, which are left in a nonequilibrium state (i.e., generation of phonons takes place). This situation, along with the low energy barrier, leads to a significant increase in the relaxation probability, as occurs during thermal heating.

This model allows us to explain the following features of the electron-induced surface reconstruction: the threshold dependence of the radiation sensitivity on electron energy, the resonance form of this energy dependence for the electron-induced structural order-disorder transition that occurs at the (001) surface of the high-temperature superconductor $\text{Bi}_2\text{Sr}_2\text{CaCu}_2\text{O}_x$, and the fact that the degree to which the electron beam affects the surface depends exponentially on the radiation dose.

Because the electronic excitation of an atom has a threshold energy dependence, the sensitivity of the electron-induced surface ordering has the same dependence. The exponential dependence of the electron beam effectiveness on the irradiation dose is a natural consequence of the model proposed here. Using this model, it is possible to explain the unusual energy dependence of the electron-induced structural order-disorder transition at the (001) surface of the high-temperature superconductor $\text{Bi}_2\text{Sr}_2\text{CaCu}_2\text{O}_x$ in the following way. Atoms are excited as a result of their interaction with electrons. There are two threshold values for the energy: a lower threshold of $\sim 10 \text{ eV}$, corresponding to the excitation of electrons that are weakly bound to the nucleus, and a higher threshold of $\sim 100 \text{ eV}$ corresponding to excitation of deeper internal electronic shells. In the process of atomic relaxation, excitation of states of the external electrons leads only to the formation of structural defects on the surface, which mediate a transition of the structure to a metastable state. In the process of atomic relaxation with excitation of the internal electronic states, these defects are annihilated.

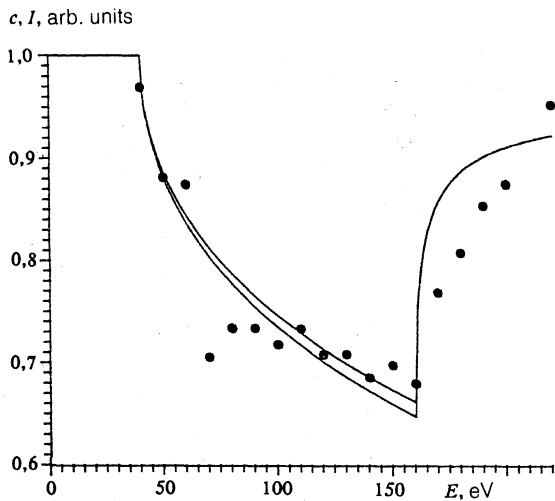


FIG. 6. Amplitude of superlattice reflection (02/5) after electron irradiation at a fixed dose on the energy of the irradiating electrons. In these measurements the amplitudes of the reflection before irradiation was the same.

Both these processes differ not only in their excitation thresholds but also in their scattering cross sections.

Let us characterize the perfection of the lattice in terms of the concentration of regular nodes c . Then if we take the defect concentration to equal $1 - c$, it is natural to assume that for specified cross sections for defect creation σ^+ and annihilation σ^- , a flux of electrons $\Delta\Phi$ causes a change in the concentration $\Delta c = -\sigma^+ c \Delta\Phi + \sigma^- (1 - c) \Delta\Phi$. In this case, for an initially perfect structure (i.e., $c = 1$ for $\Phi = 0$) the dependence of the defect concentration on the electron energy E and irradiation dose Φ has the form $c(E, \Phi) = \sigma^-(E) / \sigma^+(E) + \sigma^-(E) + \sigma^+(E) / \sigma^+(E) + \sigma^-(E) \times \exp\{-[\sigma^-(E) + \sigma^+(E)]\Phi\}$. For a fixed radiation dose, the dependence of the structural imperfection on electron energy has a form analogous to that observed experimentally (see Fig. 6). In Fig. 6, along with calculations (solid curves) we show how the efficiency of superlattice disruption depends on the energy of the irradiating electrons¹⁰ (the circles). Along the ordinate we plot the relative reflection amplitude after electron irradiation with a fixed dose, while along the abscissa we plot electron energy. In these calculations we have assumed that the energy dependence of the scattering cross section has a form characteristic of scattering processes with an energy threshold, near which $\sigma = 0$ for $E < E_0$, and $\sigma = \sigma_0(E - E_0)^{1/2}$ for $E > E_0$ (Ref. 14), where E_0 is the value of the threshold. The parameters of the calculation are as follows: the lower threshold is 40 eV, the upper threshold is 160 eV, and the scattering cross sections are taken to be $\sigma_0^+ = 1/20 \sigma_0^-$ and $\sigma_0^- \Phi = 0.8$, respectively. In order of magnitude, we have $\sigma_0^- \leq 10^{-16} \text{ cm}^2$. In

the figure we show how the shape of the curves changes with Φ . For the curves given here, the change in Φ was 5%.

Of course, we have no real proof that this model is valid. In order to verify it, the most important question to answer is: what atoms must be excited in order that defects either form or be annihilated, and why? The answers to these questions require additional investigations. However, we can identify a number of factors that might determine the degree to which atoms participate in the process. The binding energies of electrons in the various atoms that make up the lattice lie in the energy range up to 650 eV in which the surface reconstruction takes place. These energies are listed in the table of Ref. 15. Here we have taken the Fermi level to be zero in measuring the binding energies. By using Auger spectroscopy, it was established previously that cleavage of single crystals of $\text{Bi}_2\text{Sr}_2\text{CaCu}_2\text{O}_x$ takes place along planes that separate weakly bound oxygen-bismuth planes.² Thus, the surface is a BiO plane followed by CuO and SrO planes, and the diffraction pattern is primarily determined by the structure of the bismuth planes. Apparently, disordering of the positions of oxygen or bismuth atoms also causes the structural reconstruction. Both these elements have energy levels around 40 eV (see Table I). All other conditions being equal, disordering of the oxygen structure is more probable because an atom of oxygen possesses a smaller mass than an atom of bismuth, and thus acquires more energy during adiabatic relaxation. If the excitation of an atom determines the relaxation process of the surface, the fact that the threshold energy for this process is ~ 160 eV implies that such an atom cannot be either an O atom or a Ca atom (see Table I). The possibility of Bi, Sr, and Cu (which have masses 83, 38, and 29, respectively) participating in the process is not excluded. Attenuation of the electron beam, due in particular to inelastic energy losses, causes the efficiency of electronic excitation to be a maximum for bismuth and a minimum for copper. It seems to be impossible to determine unambiguously which electronically excited atoms determine the electron-induced process of surface ordering without carrying out an exact theoretical calculation. We note, however, two more circumstances that argue in favor of bismuth, both due to its large mass. First of all, bismuth has the largest effective cross section; secondly, momentum is efficiently transferred from it to other lighter atoms. The low activation energy of the disordering (or ordering) process facilitates the increase in probability of the electron-induced ordering.

The authors of Ref. 10 explained the resonant form of the energy dependence of the sensitivity for the electron-induced structural order-disorder transition on the (001) surface of the high-temperature superconductor $\text{Bi}_2\text{Sr}_2\text{CaCu}_2\text{O}_x$ in terms of a competition between two processes: electron-induced desorption of oxygen, and electron-induced diffusion of oxygen from the bulk to the surface. Apparently this model is incorrect: first of all because the

TABLE I.

Element	Energy, eV
O	24, 27, 532
Ca	26, 44, 347, 350, 438
Cu	2, 74, 120
Sr	20, 38, 133, 135, 269, 280, 358
Bi	3, 8, 25, 27, 93, 117, 158, 160, 163, 440, 464

threshold energy for electron-induced diffusion should be more than 1000 eV,¹⁾ whereas the observed threshold is in fact an order of magnitude smaller than this; and secondly, because this model cannot explain the experimentally observed exponential time dependence for the establishment of the diffraction pattern by the electron beam (Fig. 3a). Apparently the slow degradation of the diffraction pattern under irradiation by electrons with energies 200 to 650 eV (see above) is a manifestation of the process of electron-induced desorption of oxygen. The effective cross section for this process is found to be more than an order of magnitude smaller (and characteristic of this type of process; see Ref. 13) than the observed effective cross section for electron-induced reconstruction under irradiation of the surface by electrons with energies 30 to 200 eV.

The author is grateful to N. P. Tsoi for designing the mathematical algorithms and programs to control the apparatus, to S. I. Bozhko for technical assistance, and to S. G. Karabyshev for preparing the crystals of the high-temperature superconductor $\text{Bi}_2\text{Sr}_2\text{CaCu}_2\text{O}_x$.

¹⁾B. M. Shepelevski, private communication.

¹⁾P. A. P. Lindberg, Z. -X. Shen, B. O. Wells, D. B. Mitzi, I. Lindau, W. E. Spicer, and A. Kapitulnik, *Appl. Phys. Lett.* **53**, 2563 (1988).

- ²⁾S. Nakanishi, N. Fukuoka, K. Nakahigashi, M. Kogachi, H. Sasakura, S. Minagimawa, and A. Yanase, *Jpn. J. Appl. Phys.* **28**, N1, L71 (1989).
- ³⁾R. Claessen, R. Manzke, H. Carstensen, B. Burandt, T. Buslaps, M. Skibowski, and J. Fink, *Phys. Rev. B* **39**, 37 (1989).
- ⁴⁾S. Kishida, H. Tokutaka, S. Nakanishi, K. Nishimori, N. Ishihara, and H. Fijimoto, *Jpn. J. Appl. Phys.* **28**, N3, L406 (1989).
- ⁵⁾S. Kishida, H. Tokutaka, H. Fijimoto, K. Nishimori, and N. Ishihara, *Jpn. J. Appl. Phys.* **28**, N8, L1389 (1989).
- ⁶⁾I. B. Al'tfeder, A. P. Volodin, V. A. Grazhulis, A. M. Ionov, Karabashiev, Pis'ma Zh. Eksp. Teor. Fiz. **50**, 182 (1989) [*JETP Lett.* **50**, 204 (1989)].
- ⁷⁾M. D. Dirk, C. B. Eom, B. Oh, S. P. Spielman, M. R. Beasley, A. Kapitulnik, T. H. Geballe, and C. F. Quate, *Appl. Phys. Lett.* **52**, 2071 (1988).
- ⁸⁾M. D. Dirk, J. Nogami, A. A. Baski, D. B. Mitzi, A. Kapitulnik, T. H. Geballe, and C. F. Quate, *Science* **242**, 1673 (1988).
- ⁹⁾C. K. Shih, R. M. Feenstra, J. R. Kirtley, and G. V. Chandrasekhar, *Phys. Rev. B* **40**, N4, 2682 (1989).
- ¹⁰⁾S. I. Bozhko and V. S. Tsoi, *Physica C* **197**, 362 (1992).
- ¹¹⁾A. M. Balbashev *et al.*, *Sverkhprovodimost': fizika, khimiya, tekhnika* (Superconductivity: Physics, Chemistry, Engineering) **2**, N1, 57 (1989).
- ¹²⁾A. A. Moskalev and V. S. Tsoi, *Poverkhnost' fizika, khimiya, mekhanika* (The Surface: Physics, Chemistry, Mechanics) **5**, 52 (1985).
- ¹³⁾M. L. Knotek, *Rep. Prog. Phys.* **47**, 1499 (1984).
- ¹⁴⁾L. D. Landau and E. M. Lifshits, *Quantum Mechanics*, 3rd ed., Pergamon, Oxford (1977).
- ¹⁵⁾K. Zigban, K. Kordlung, A. Fal'man *et al.*, *Electron Spectroscopy* (in Russian), Mir, Moscow, 1989.

Translated by Frank J. Crowne